



ELSEVIER

Available online at www.sciencedirect.com

SCIENCE @ DIRECT®

Journal of Magnetism and Magnetic Materials 262 (2003) 445–451

www.elsevier.com/locate/jmmm

Magnetization reversal in weak ferrimagnets and canted antiferromagnets

H. Kageyama^a, D.I. Khomskii^b, R.Z. Levitin^c, M.M. Markina^c, T. Okuyama^d,
T. Uchimoto^d, A.N. Vasil'ev^{c,*}

^a *Materials Design and Characterization Laboratory, Institute for Solid State Physics, University of Tokyo, 5-1-5 Kashiwanoha, Kashiwa, Chiba 277-8581, Japan*

^b *Solid State Physics Laboratory, Materials Science Center, University of Groningen, Nijenborgh 4, 9747 AG Groningen, The Netherlands*

^c *Physics Faculty, Moscow State University, Moscow 119899, Russia*

^d *Institute of Fluid Science, Tohoku University, Katahira 2-1-1, Aoba-ku, Sendai 980-8577, Japan*

Abstract

In some ferrimagnets the total magnetization vanishes at a certain compensation temperature T^* . In weak magnetic fields, the magnetization can change sign at T^* (the magnetization reversal). Much rarer is observation of ferrimagnetic-like response in canted antiferromagnets, where the weak ferromagnetic moment is due to the tilting of the sublattice magnetizations. The latter phenomenon was observed in nickel (II) formate dihydrate $\text{Ni}(\text{HCOO})_2 \cdot 2\text{H}_2\text{O}$. The observed weak magnetic moment increases initially below $T_N = 15.5$ K, equals zero at $T^* = 8.5$ K and increases again at lowering temperature. The sign of the low-field magnetization at any given temperature is determined by the sample's magnetic prehistory and the signs are opposite to each other at $T < T^*$ and $T^* < T < T_N$.

© 2003 Elsevier Science B.V. All rights reserved.

PACS: 75.50.Gg; 75.60.Jk

Keywords: Weak ferrimagnetism; Compensation point; Magnetization reversal; $\text{Ni}(\text{HCOO})_2 \cdot 2\text{H}_2\text{O}$

The phenomena of ferrimagnetism are associated with a partial cancellation of antiferromagnetically aligned magnetic sublattices with different values of magnetic moments and/or different temperature dependencies of magnetization. It is well studied in ferrites [1] and recently in various inorganic [2,3] and molecular transition metal complexes [4,5]. Ferrimagnetic behaviour is observed frequently in compounds containing different magnetic ions. It can be seen also in materials containing only one type of magnetic ions, which are in different valence states or crystallographic positions [6,7]. In the latter case the origin of ferrimagnetism lies in the difference of molecular fields acting on non-equivalent magnetic sites.

In some ferrimagnets (in Néel's classification N-type ferrimagnets [8]) the total magnetization of a substance vanishes at a certain compensation temperature T^* . Both above and below this temperature the magnetization of different sublattices prevails. In this case magnetization reversal can be observed. In a weak magnetic field (less than the field of coercivity) the magnetization changes sign at the compensation

*Corresponding author.

E-mail address: vasil@mig.phys.msu.ru (A.N. Vasil'ev).

temperature. The metastable “diamagnetic” state can be fixed by the magnetocrystalline anisotropy in a certain temperature range.

Much rarer is the observation of ferrimagnetic-like response in canted antiferromagnets, where a weak ferromagnetic moment is due to the tilting of sublattice magnetizations. The single-ion magnetic anisotropy itself is able to fix the directions of sublattice magnetizations tilted from antiparallel alignment [9]. On the other hand, the canting of antiferromagnetic sublattices can be due to the antisymmetric Dzyaloshinsky–Moriya interaction [10–12], which favours perpendicular orientations of the sublattice magnetizations. Very few canted antiferromagnets show a compensation point and magnetization reversal [13–15].

We report the observation of weak ferrimagnetism, compensation point and magnetization reversal in nickel (II) formate dihydrate $\text{Ni}(\text{HCOO})_2 \cdot 2\text{H}_2\text{O}$. This compound crystallises in the monoclinic $\text{P2}_1/\text{c}$ space group, and includes four formula units in the unit cell with $a = 8.60 \text{ \AA}$, $b = 7.06 \text{ \AA}$, $c = 9.21 \text{ \AA}$, $\beta = 96.5^\circ$ [16]. The structure contains two kinds of Ni^{2+} ions: the Ni_1 with six oxygen of different formate ions as nearest neighbors, the Ni_2 with four water molecules and two formate oxygen coordinated. In both Ni_1 and Ni_2 subsystems the octahedrons coordinating the Ni ions are tilted with respect to each other. The fourfold axes of NiO_6 octahedrons are oriented differently with respect to the crystal lattice axes. The crystal structure of $\text{Ni}(\text{HCOO})_2 \cdot 2\text{H}_2\text{O}$ in polyhedral NiO_6 representation is shown in Fig. 1. In Ni_1 subsystem the fourfold axes lie mainly in a – b crystal plane and are tilted over $\psi_1/2 = 22.5^\circ$ in opposite directions from the a -axis. In the Ni_2 subsystem the fourfold axes also lie mainly in the a – b plane and are tilted over $\psi_2/2 = 57.5^\circ$ from the a -axis.

Magnetic properties of commercially available (Waco Co.) powder samples of $\text{Ni}(\text{HCOO})_2 \cdot 2\text{H}_2\text{O}$ were measured in a “Quantum Design” SQUID magnetometer in 2–300 K temperature range, in fields up to 7 T. X-rays analysis confirmed the single phase of the title compound in the measured sample.

The temperature dependencies of the magnetization, expressed as M/H , of a $\text{Ni}(\text{HCOO})_2 \cdot 2\text{H}_2\text{O}$ powder sample taken in zero-field-cooling (ZFC) and field-cooling (FC) regimes at $H = 0.01 \text{ T}$ are shown in Fig. 2. At heating in the ZFC regime, the sample shows firstly a large “paramagnetic” response at low temperatures. Then, the magnetic moment gradually decreases with increasing temperature, changes to “diamagnetic” at $T^* = 8.5 \text{ K}$, and once again becomes paramagnetic above 15.5 K. At subsequent cooling in the FC regime, the magnetic response of the sample at low temperatures shows mirror-like behaviour with respect to the magnetization sign as compared with ZFC measurements. The temperature dependence

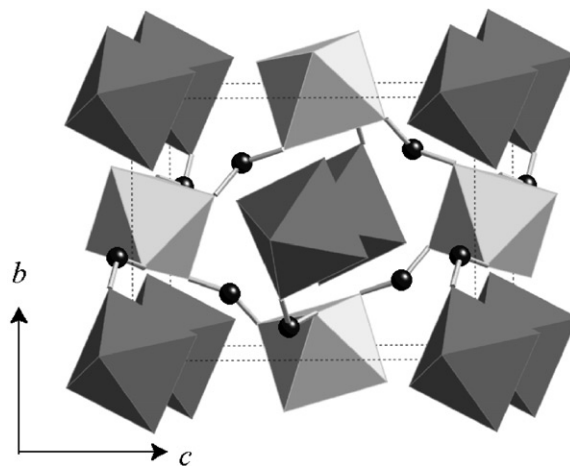


Fig. 1. Crystal structure of $\text{Ni}(\text{HCOO})_2 \cdot 2\text{H}_2\text{O}$ in polyhedral NiO_6 representation. Light-shaded octahedrons belong to the Ni_1 subsystem, and dark-shaded octahedrons belong to the Ni_2 subsystem. The C ions are shown by black circles and the pathways of exchange interaction Ni-O-C-O-Ni are shown by solid lines.

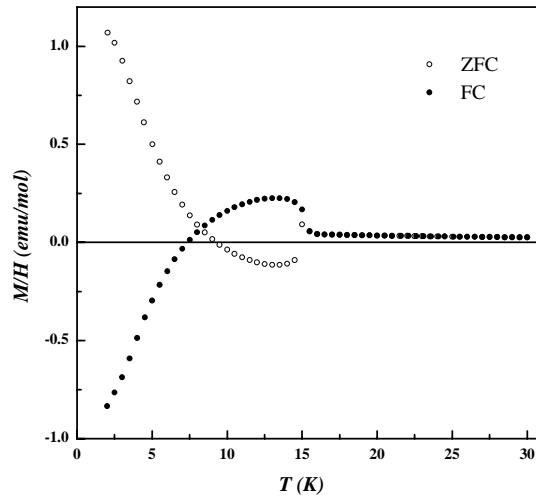


Fig. 2. Temperature dependence of the magnetization, expressed as M/H , of $\text{Ni}(\text{COOH})_2 \cdot 2\text{H}_2\text{O}$ at $H = 0.01$ T taken in ZFC (\circ) and FC (\bullet) regimes.

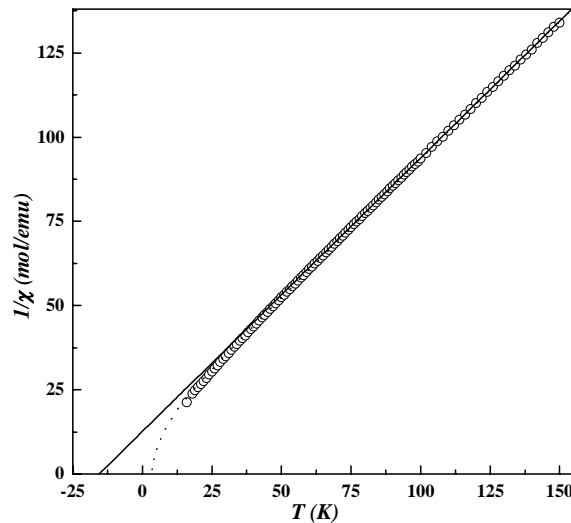


Fig. 3. Inverse magnetic susceptibility of $\text{Ni}(\text{HCOO})_2 \cdot 2\text{H}_2\text{O}$ at $T > T_N$. The solid line represents the linear extrapolation from the high temperature region. The dotted line represents the numerical fit by Eq. (5).

of the inverse susceptibility χ^{-1} of $\text{Ni}(\text{HCOO})_2 \cdot 2\text{H}_2\text{O}$ at $T > T_N$ is shown in Fig. 3. At high temperatures χ follows the Curie–Weiss law with paramagnetic Curie temperature $\Theta = -15.5$ K and effective magnetic moment $\mu_{\text{eff}} = 3.14 \mu_B$. This value of μ_{eff} is a typical one for a magnetic moment of Ni^{2+} ions. The negative value of Θ implies that the main exchange interaction in $\text{Ni}(\text{HCOO})_2 \cdot 2\text{H}_2\text{O}$ is antiferromagnetic.

The magnetization curves taken in the ZFC regime at $T < T_N$ are shown in Fig. 4. These curves are ferromagnetic-like, i.e. they show spontaneous magnetic moments, are weakly non-linear at low fields and tend to linear dependencies at high magnetic fields. Note that the absolute values of the magnetization are by two orders of magnitude smaller than those corresponding to a parallel alignment of the Ni^{2+} magnetic

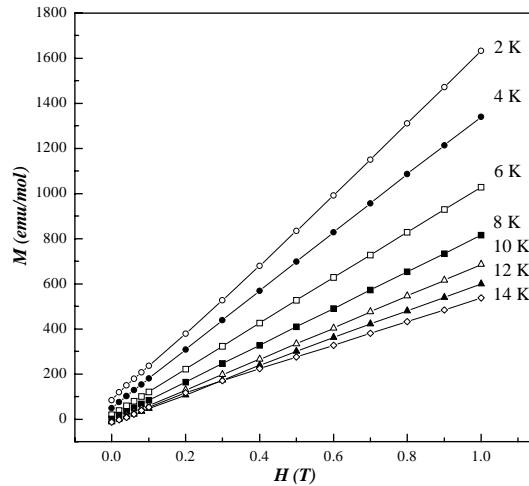


Fig. 4. Magnetization curves of $\text{Ni}(\text{COOH})_2 \cdot 2\text{H}_2\text{O}$ taken in the ZFC regime at $T < T_N$.

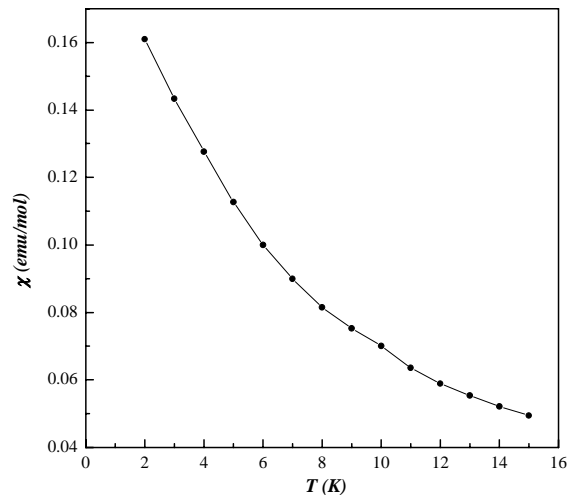


Fig. 5. Temperature dependence of the high-field magnetic susceptibility of $\text{Ni}(\text{HCOO})_2 \cdot 2\text{H}_2\text{O}$ at $T < T_N$.

moments. The temperature dependence of the high-field magnetic susceptibility χ in the magnetic ordered state, obtained from the slope of the magnetization curves at high fields, is shown in Fig. 5.

Therefore, the experimental data presented suggest that below $T_N = 15.5 \text{ K}$ a weakly ferrimagnetic state is established in $\text{Ni}(\text{HCOO})_2 \cdot 2\text{H}_2\text{O}$, and that $T^* = 8.5 \text{ K}$ is a compensation temperature.

According to crystal structure considerations the superexchange pathways between Ni ions can be realized through Ni–O–C–O–Ni links. As noted earlier, both the Ni_1 and the Ni_2 subsystem contain two kinds of Ni ions with different orientations of octahedral environments. Consequently, it is natural to represent each Ni subsystem as consisting of two sublattices, namely Ni_1' , Ni_1'' and Ni_2' , Ni_2'' . The superexchange Ni–O–C–O–Ni links exist between Ni_1' and Ni_1'' and also between Ni_1' and Ni_2' , and Ni_1'' and Ni_2'' . Therefore, each Ni_1' ion interacts with four nearest neighboring Ni_1'' ions and two nearest

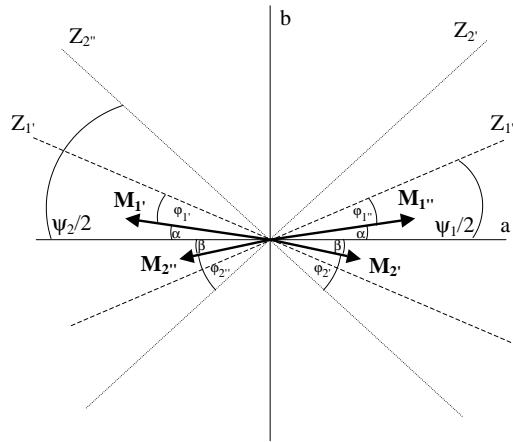


Fig. 6. The model for the weak ferrimagnetic structure of $\text{Ni}(\text{HCOO})_2 \cdot 2\text{H}_2\text{O}$. The magnetic moments $M_{1'}$, $M_{1''}$, $M_{2'}$, $M_{2''}$ of different Ni ions are assumed to lie in the a - b plane. The dotted lines show the orientations of the principal axes (easy directions of magnetization) $Z_{1'}$, $Z_{1''}$, $Z_{2'}$, $Z_{2''}$ of different NiO_6 octahedrons. The angles between these easy directions and the a axis are $\psi_{1'} = \psi_{1''} = \psi_1$ and $\psi_{2'} = \psi_{2''} = \psi_2$. The deviations from antiparallel alignment of magnetic moments within the Ni_1 and Ni_2 subsystems are designated as α and β , respectively. The angles $\phi_{1'} = \phi_{1''} = \phi_1$ and $\phi_{2'} = \phi_{2''} = \phi_2$ give the deviations of the corresponding magnetic moments from the easy directions of magnetization.

neighboring Ni_2' ions. The same is true for Ni_1'' ions. The pathway parameters, i.e. the interatomic distances and angles, for all the superexchange interactions mentioned are close to each other. There are no Ni–O–C–O–Ni superexchange pathways within the Ni_2 subsystem. It means that in the absence of Ni_1 – Ni_2 exchange interactions the Ni_2 subsystem can be considered paramagnetic down to the lowest temperatures. The superexchange pathways are shown in Fig. 1 by solid lines. The crystal field fixes the orientations of different Ni magnetic moments in different directions with respect to the crystallographic axes and results in the tilting of these moments from antiparallel alignment.

The properties of $\text{Ni}(\text{HCOO})_2 \cdot 2\text{H}_2\text{O}$ in the framework of the model suggested can be described using the following expression for a free energy:

$$E = 4IM_{1'}M_{1''} + 2I(M_{1'}M_{2'} + M_{1''}M_{2''}) + K_{\text{Ni}1} \sin^2 \phi_1' + K_{\text{Ni}1} \sin^2 \phi_1'' + K_{\text{Ni}2} \sin^2 \phi_2' + K_{\text{Ni}2} \sin^2 \phi_2'' - M(M_{1'} + M_{1''} + M_{2'} + M_{2''}). \quad (1)$$

Here, I is the exchange interaction coefficient, $|M_{1'}| = |M_{1''}| = M_1$ and $|M_{2'}| = |M_{2''}| = M_2$ are the magnetic moments of the Ni_1 and Ni_2 sublattices. The first term in Eq. (1) describes the exchange interactions within the Ni_1 subsystem. The second term describes the exchange interactions between the Ni_1 and Ni_2 subsystems and these interactions are assumed to be the same on the basis of crystal lattice considerations. The next four terms describe of the magnetic anisotropy. The angles $\phi_1' = \phi_1'' = \phi_1$ and $\phi_2' = \phi_2'' = \phi_2$ are the angles between the easy axes of magnetization and the magnetic moments of the corresponding Ni ions. It is natural to assume that the easy axes of magnetization coincide with the principal axes of the NiO_6 octahedrons. The last term in Eq. (1) is a Zeeman energy.

The minimization of Eq. (1) with respect to ϕ_1 and ϕ_2 gives the equilibrium orientations of the Ni magnetic moments. It was found that these moments lie in the a - b plane and are oriented as shown in Fig. 6. According to this arrangement each Ni subsystem is weakly ferromagnetic and these weakly ferromagnetic moments are oriented antiparallel to each other. Therefore, the resulting magnetic structure of $\text{Ni}(\text{HCOO})_2 \cdot 2\text{H}_2\text{O}$ is a weakly ferrimagnetic one. In the assumption that the crystal field energy for Ni

ions is much smaller than the exchange interaction, the deviations from the antiparallel alignment will be small. In the Ni₁ and Ni₂ subsystems these deviations will be denoted α and β , respectively.

The temperature dependencies of the sublattice magnetizations M_1 and M_2 can be calculated within the exchange approximation through the corresponding Brillouin functions B_S :

$$M_1 = gS\mu_B B_S[IgS\mu_B(4M_1 + 2M_2)/k_B T], \quad (2)$$

$$M_2 = gS\mu_B B_S[IgS\mu_B(2M_1)/k_B T], \quad (3)$$

where g is a g -factor, spin $S = 1$ is the spin of a Ni²⁺ ion. These and forthcoming expressions are given for a formula unit.

Eqs. (2) and (3) allow to calculate the Néel temperature

$$T_N = \frac{2CI}{\sqrt{2} - 1}, \quad (4)$$

where $C = g^2 S(S+1)\mu_B^2/3k_B$.

The magnetic susceptibility χ at $T > T_N$ is

$$\chi = \frac{C}{T + 4CI - 4C^2 I^2 / T}. \quad (5)$$

Clearly, χ deviates from the Curie–Weiss law approaching the Néel temperature which reflects the presence of two different magnetic subsystems in Ni(COOH)₂·2H₂O. The inverse paramagnetic susceptibility is extrapolated down to zero at the paramagnetic Curie point

$$\Theta' = -2CI(1 - \sqrt{2}). \quad (6)$$

In the exchange approximation, it is possible also to calculate the magnetic susceptibility in the magnetic ordered state at $T < T^N$:

$$\chi = \frac{(1+m)^2}{16I}, \quad (7)$$

where $m = M_2/M_1$. Note that the temperature dependence of χ is not trivial. χ increases at lowering temperature due to the fact that the Ni₂ subsystem itself is paramagnetic in the absence of exchange interactions with the Ni₁ subsystem. Indeed, this behaviour was observed experimentally, as shown in Fig. 5.

To calculate the weak ferromagnetic moment of Ni(HCOO)₂·2H₂O at $T < T_N$, it is necessary to step out beyond the frames of the exchange approximation and to take the magnetic anisotropy into account. The minimization of the free energy (1) at $H = 0$ allows to obtain the deviations of the magnetic moments α and β from antiparallel alignment within both the Ni₁ and Ni₂ subsystems, and to calculate the resulting weak ferrimagnetic moment

$$M_{\text{total}} = M_1(a - m\beta)/2 \quad (8)$$

or

$$M_{\text{total}} = \frac{M_1}{2} \frac{2q_1 q_2 \sin \psi_1 \cos \psi_2 + m(q_1 \sin \psi_1 - 3q_2 \sin \psi_2 - 2q_1 q_2 \cos \psi_1 \sin \psi_2) - m^2(q_1 \sin \psi_1 + q_2 \sin \psi_2)}{m(4 + 2q_1 \cos \psi_1 + q_2 \cos \psi_2) + 8q_2 \cos \psi_2 + 4q_1 q_2 \cos \psi_1 \cos \psi_2}. \quad (9)$$

The angles ψ_1 and ψ_2 are the angles between the easy axes of magnetization within the Ni₁ and Ni₂ subsystems, $q_1 = K_{\text{Ni1}}/2IM_1^2$, $q_2 = K_{\text{Ni2}}/2IM_1^2$.

The experimental data available for Ni(HCOO)₂·2H₂O can be compared with results of analytical and numerical calculations within the model proposed. The exchange interaction coefficient $I = 1.77 \text{ T}/\mu_B$ was

calculated from formula (4) for the Néel temperature. In this model the value of the paramagnetic Curie temperature $\Theta' = 2.6$ K (see Eq. (6)). The magnetic susceptibility at $T > T_N$ in this model is given by Eq. (5) and experimental data could be well fitted by the theoretical curve shown by the dotted line in Fig. 3. The paramagnetic Curie temperature found through the fitting procedure $\Theta' = 3.5$ K is close to that calculated within the model approximation.

The physical scenario for the appearance of a compensation for $\text{Ni}(\text{HCOO})_2 \cdot 2\text{H}_2\text{O}$ looks as follows. At cooling below the Néel temperature, the weak magnetization of the Ni_1 subsystem exceeds that of the Ni_2 subsystem. This occurs because the $M_1(T)$ dependence is much steeper than the $M_2(T)$ dependence in the vicinity of T_N . It results in an initial increase of the total magnetization M_{total} below T_N . At further cooling, the magnetization values of the Ni_1 and Ni_2 subsystems approach each other and compensation of their magnetizations occurs at T^* . If the magnetic anisotropy in the Ni_2 subsystem is “larger” than that in the Ni_1 subsystem, at low temperatures the weak magnetization of the Ni_2 subsystem will prevail.

Concluding, the phenomenon of weak ferrimagnetism is found in nickel (II) formate dihydrate $\text{Ni}(\text{HCOO})_2 \cdot 2\text{H}_2\text{O}$ containing only one type of magnetic ions. These ions constitute two canted antiferromagnetic subsystems whose competition results in a compensation point and magnetization reversal. This observation widens the range of the substances and of the physical mechanisms responsible for the appearance of a compensation point and magnetization reversal in weakly ferrimagnetic compounds.

This work was supported by NWO Grant 047-008-012.

References

- [1] S. Krupichka, Physik der Ferrite und der Verwandten Magnetischen Oxide, Academia, Prag, 1973.
- [2] N. Menyuk, K. Dwight, D.G. Wickham, Phys. Rev. Lett. 4 (1960) 119.
- [3] N. Sakamoto, Y. Yamaguchi, J. Phys. Soc. Jpn. 17 (Suppl. B1) (1962) 276.
- [4] C. Mathoniere, C.J. Nuttall, S.G. Carlong, P. Day, Inorg. Chem. 35 (1996) 1201.
- [5] N. Re, E. Gallo, C. Floriani, H. Miyasaka, N. Matsumoto, Inorg. Chem. 35 (1996) 5964.
- [6] N. Shirakawa, M. Ishikawa, Jpn. J. Appl. Phys. 30 (1991) L755.
- [7] A.V. Mahajan, D.C. Johnston, D.R. Torgesen, F. Borsa, Phys. Rev. B 46 (1992) 10966.
- [8] L. Neel, Ann. Phys. (Leipzig) 3 (1948) 137.
- [9] T. Moriya, Weak ferromagnetism, in: G.T. Rado, H. Suhl (Eds.), Ferromagnetism, Vol. 1, New York, London, 1963.
- [10] I. Dzyaloshinsky, J. Phys. Chem. Solids 4 (1958) 241.
- [11] T. Moriya, Phys. Rev. 117 (1960) 635.
- [12] T. Moriya, Phys. Rev. 120 (1960) 91.
- [13] Y. Ren, T.T.M. Palstra, D.I. Khomskii, E. Pellegrin, A.A. Nugroho, A.A. Menovsky, G.A. Sawadzky, Nature 396 (1998) 441.
- [14] Y. Ren, T.T.M. Palstra, D.I. Khomskii, E. Pellegrin, A.A. Nugroho, A.A. Menovsky, G.A. Sawadzky, Phys. Rev. B 62 (2000) 6577.
- [15] A.M. Kadomtseva, A.S. Moskvina, I.G. Bostrem, B.M. Vanklin, N.A. Hafizova, JETP 72 (1977) 2286.
- [16] von K.Krogmann, R. Mattes, Z. Kristallogr. 118 (1963) 291.